Anal Bioanal Chem (2014) 406:7463–7471
DOI 10.1007/s00216-014-8185-x

RESEARCH PAPER

Determination of major nonmetallic impurities in magnesium by glow discharge mass spectrometry with a fast flow source using sintered and pressed powder samples

Alexei Plotnikov · Jens Pfeifer · Silke Richter · Heinrich Kipphardt · Volker Hoffmann

Received: 28 March 2014 / Revised: 11 September 2014 / Accepted: 12 September 2014 / Published online: 12 October 2014

Abstract Fast flow glow discharge mass spectrometry with a Grimm-type ion source providing a high sputter rate was used for the determination of major nonmetallic impurities in magnesium. The analytical signal was found to be strongly influenced by the electrical discharge parameters. For calibration by standard addition, synthetic standard samples were produced in two different ways—namely, by pressing and by sintering doped metal powders. The observed sensitivity of the calibration curves was shown to depend on the particle size of the powder. For the magnesium powders, the mass fractions of oxygen, nitrogen, boron, and silicon were determined to be about 0.01 $kg \cdot kg^{-1}$ (relative standard deviation approximately 10–20 %), 2,700 $mg \cdot kg^{-1}$, 150 $mg \cdot kg^{-1}$, and 300 $mg \cdot kg^{-1}$, respectively.

Keywords Glow discharge mass spectrometry · Magnesium matrix · Nonmetallic impurities · Fast flow source · Electrical parameters · Calibration samples

Introduction

Magnesium is widely used in industrial lightweight construction alloys [1]. However, the presence of nonmetallic inclusions, e.g., in the form of oxides or silicides, has a significant influence on the machinability and surface quality of magnesium and its alloys [2]. Owing to the high oxidation potential of magnesium as compared with aluminum [3] as well as the poor protection properties of the natural surface oxide layer, even bulk refined magnesium can contain oxygen contents of up to several hundred milligrams per kilogram [4]. Silicon as another major nonmetallic impurity in magnesium results from the use of ferrosilicon in the production process. The control of such nonmetallic impurities by means of an efficient analytical method is of critical importance for the production of magnesium materials with the desired quality or properties. Moreover, such a method is also attractive for other applications, such as the determination of the total purity, which is needed to establish primary calibration standards for element determination. However, the determination of nonmetallic impurities in magnesium and its alloys is still a challenge for modern analytical chemistry.

The methods currently used for the determination of oxygen in magnesium [5] can be divided into two groups. The first group consists of methods that determine oxygen directly, regardless of its chemical form. Examples for this group are activation analysis with fast neutrons or with charged particles [6], inert gas fusion with infrared absorption [4], and glow discharge (GD) spectrometry [7]. The second group of methods determine oxygen indirectly via the content of the MgO. Examples for this type are quantitative metallography [8] and optical measurements [9]. However, all these methods have certain limitations. The application of activation analysis with fast neutrons or with charged particles is limited by the availability of an activation device such as a nuclear reactor or a charged particle accelerator. Measuring oxygen in magnesium by inert gas fusion with infrared absorption is experimentally difficult, because the reduction of MgO by carbon requires a temperature as high as 2,700 °C, which significantly exceeds the boiling point of magnesium (1,090 °C). Intensive sample evaporation results in gettering of the released CO.

Published in the topical collection *Emerging Concepts and Strategies in Analytical Glow Discharges* with guest editors Rosario Pereiro and Steven Ray.

A. Plotnikov (✉) · J. Pfeifer · S. Richter · H. Kipphardt
BAM Federal Institute for Materials Research and Testing,
Richard-Willstätter-Str. 11, 12489 Berlin, Germany
e-mail: alexei.plotnikov@gmx.de

V. Hoffmann
Leibniz Institute for Solid State and Materials Research Dresden,
Postfach 27 01 16, 01171 Dresden, Germany

Therefore, matrix separation by distillation is required [4] to avoid an underestimation of the oxygen content. Methods based on optical examination of the sample surface or metallographic analysis of the MgO phase after dissolution and filtration are limited by relatively high detection limits and low accuracy.

GD optical emission spectrometry (OES) and GD mass spectrometry (MS) are powerful methods not only for the determination of both metallic and nonmetallic bulk impurities in magnesium and its alloys [10, 11], but also for semi-quantitative depth profiling as applied for the oxygen content in magnesium alloys [12].

However, the detection capabilities provided by commercial GD-OES instruments without specific optimization for high sensitivity in the vacuum UV region are not sufficient for the determination of oxygen in purified magnesium (V. Hoffmann, personal communication). With GD-MS the situation is different: instruments with a conventional low-pressure source provide significantly higher sensitivities and are able to determine oxygen in magnesium at a level of several tens of milligrams per kilogram [7]. The application of a cryo-cooled GD cell reduces the background of carbon, oxygen, and nitrogen considerably and, hence, improves the detection limits by two to three orders of magnitude, making possible the determination of these elements in a gallium arsenide matrix at the sub-milligram per·kilogram level [13]. However, the matrix-specific relative sensitivity factors (RSFs) for the nonmetals reported for this case differ by several orders of magnitude (up to 4), which makes the use of standard RSFs (SRSFs) inadequate for quantification purposes.

Moreover, the application of a conventional GD source with low sputter rates is very time-consuming—a typical analysis takes 1–2 h. Reducing the costs by shortening the time needed for analysis was one of the main reasons for developing a "fast flow" GD source (Grimm type) with a higher pressure inside the discharge cell [14, 15]. However, the physics of a fast flow GD and, as a consequence, the formation of the analytical response can be more complex compared with the case for a conventional source [16]. For instance, the transport efficiency of the sputtered matter and also mass discrimination effects depend heavily on the local gas flow dynamics inside the GD source [17]. The latter is very difficult to observe experimentally, since placement of sensor elements inside a GD system inherently disturbs the local gas flow. Moreover, additional discharges may occur outside the usual discharge region owing to an increased pressure at the interface [16]. In fact, especially for the fast flow GD source, all parameters (gas flow rate, current, and voltage) cannot be varied independently because of their strong correlation. The concept described above has also been exploited in commercially based systems discussed in [14, 15] to form a pulsed radio-frequency GD time-of-flight MS system with a modified Grimm GD source and with sputtering rates comparable to those shown by GD-OES instruments.

The aim of this study was to examine the potential of GD-MS with a "fast flow" ion source for the determination of nonmetallic impurities (primarily oxygen) in magnesium. In addition to investigating the influence of the electrical discharge parameters for the magnesium matrix, we also investigated the applicability of pressed as well as sintered doped magnesium powders for calibration.

Experimental

Materials

Two magnesium powders of different granularity and purity (100–200 and 325 mesh with certified metallic purities of 99.6 and 99.8 %, respectively) as well as compact material (cylindrical rod, diameter 33 mm, 99.8 % metallic purity) were purchased from Alfa Aesar (Ward Hill, MA, USA; product numbers 36194, 10233, and 10231, respectively). Magnesium oxide powder was purchased from Merck (Darmstadt, Germany; product number 5866). Silicon nitride and boron nitride certified reference materials (ERM-ED101 and ERM-ED103, respectively) were available at BAM [18, 19].

Sample preparation

Magnesium oxide was used as a dopant for both pressed and sintered samples, and Si_3N_4 and a mixture of BN with Si_3N_4 and finally MgO powder were used as dopants for pressed samples only. Weighed amounts of the magnesium powder and dopant were quantitatively transferred into a polypropylene vessel (10 mL, together with a polypropylene ball) and put into a Spex 8000 Mixer/Mill (Spex Industries, Metuchen, NJ, USA) and then thoroughly homogenized for 10 min.

The homogenized powders were then pressed into a filling ring, forming a conducting pellet with a diameter of 11 mm (Fig. 1c). The setup used for pressing of the pellets from homogenized powder mixtures as well as the pressing procedures were described previously in detail by Matschat et al. [20]. The sintering of magnesium powders to compact material (Fig. 1a, b) was conducted in an argon atmosphere at 400 °C and 477 MPa. A fine magnesium powder (325 mesh) was used for the fabrication of sintered samples, whereas pressed samples were prepared in two sets of different granularity using 100–200- and 325-mesh magnesium powders for each dopant type.

Each set of calibration standards (Table 1) included three samples with different dopant content and a blank sample.

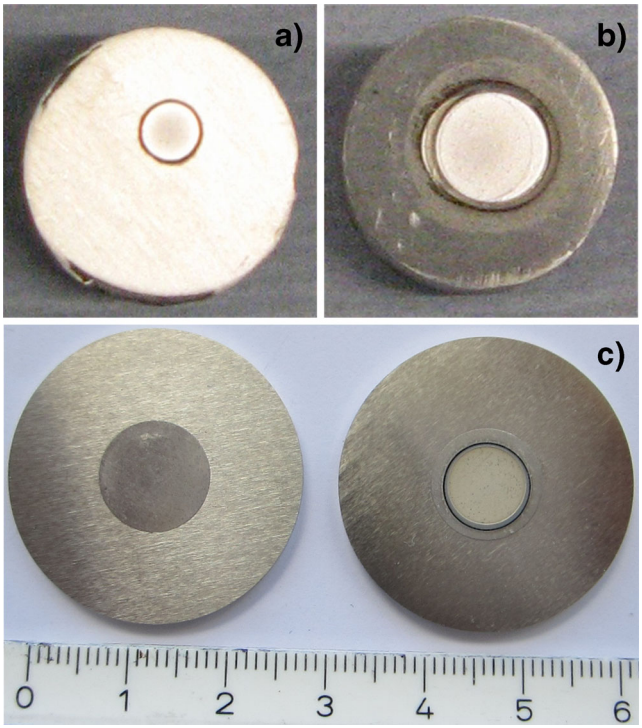

Fig. 1 Typical samples used in the study: sintered compact samples (**a**, **b**); pressed pellet in a steel ring (**c**)

Glow discharge mass spectrometry

The measurements were performed using an ELEMENT GD (Thermo Fisher Scientific, Bremen, Germany) double focusing sector field GD mass spectrometer equipped with a Grimm-type fast flow GD cell. The diameter of the sputtering area was 8 mm. Sample mounting and other details of the measurement were described in detail previously [20]. Presputtering was performed before each measurement until the analyte-to-magnesium signal intensity ratio (ion beam ratio, IBR) became stable. Measurements were performed at medium resolution ($m/\Delta m \approx 4{,}000$).

Table 1 Composition of prepared samples

325 mesh with O as MgO and pressed				
w(O) (%)	0.0	3.0	5.6	9.9
100–200 mesh with O as MgO and pressed				
w(O) (%)	0.0	3.0	5.6	9.9
325 mesh with O as MgO and sintered				
w(O) (%)	0.0	3.0	5.6	9.9
325 mesh with Si_3N_4 and BN and pressed				
w(N) (%)	0.000	0.173	0.325	0.618
w(B) (%)	0.000	0.098	0.200	0.400
w(Si) (%)	0.000	0.068	0.097	0.149
325 mesh with Si_3N_4 and BN and pressed				
w(N) (%)	0.000	0.139	0.310	0.600

A Statron 4222 external power supply (Statron, Finsterwalde, Germany) was used to provide the GD voltage for measurements in galvanostatic mode. An inductance coil (inductance $L=15$ H) was daisy-chained between the GD power supply and the cathode to prevent self-amplification of voltage oscillations as well as to reduce signal spikes.

Glow discharge optical emission spectrometry

To check the gas impermeability of the samples via the absence of molecular bands from air, a CCD-based instrument (GDA 650 from Spectruma Analytik, Hof, Germany) covering a wavelength range from 120 to 550 nm was used. Because of the higher sensitivity for homogeneity measurements, a photomultiplier-tube-based instrument (GDA 750 from Spectruma Analytik) with the following wavelengths was used: 121.6 nm (H), 130.2 nm (O), 149.3 nm (N), 156.1 nm (C), 208.9 nm (B), 219.2 nm (Cu), 327.4 nm (Cu), 288.1 nm (Si), and 415.9 nm (Ar). Owing to the sample geometry of the pressed powders, a crater diameter of 4 mm was chosen for all measurements. With a voltage of 380 V and a current of 18 mA, a gas flow rate of 190 $cm^3 \cdot s^{-1}$ was obtained. Additional tests with a crater diameter of 8 mm and fourfold current confirmed that the electrical parameters of GD-OES and GD-MS are comparable.

Results and discussion

Sample properties

The pressed pellets obtained were mechanically stable and provided sufficient electrical conductivity for direct current GD measurements. The gas impermeability and homogeneity of the different samples were confirmed by additional GD-OES measurements. GD-OES allows the detection of molecular species (air components) penetrating through a porous sample into the GD cavity. The overlay of typical spectra obtained on compact and pressed powder samples as shown in Fig. 2 showed no evidence of the presence of molecular bands, especially in the spectral region from 330 to 335 nm, indicating the gastightness of the pressed and sintered samples. Additionally, one of the most sensitive atomic lines of nitrogen, at 174.27 nm, was not observed in the monitored spectra.

Typical transient signals from the matrix and analyte obtained with GD-MS and GD-OES are compared in Fig. 3 for different samples and analytes. GD-OES provides better signal stability as needed for homogeneity measurements as can be seen in the comparison of Fig. 3 panels a–c with panel d. For the measurements displayed in Fig. 3 panel d, Si_3N_4 was chosen instead of MgO because of the low sensitivity for

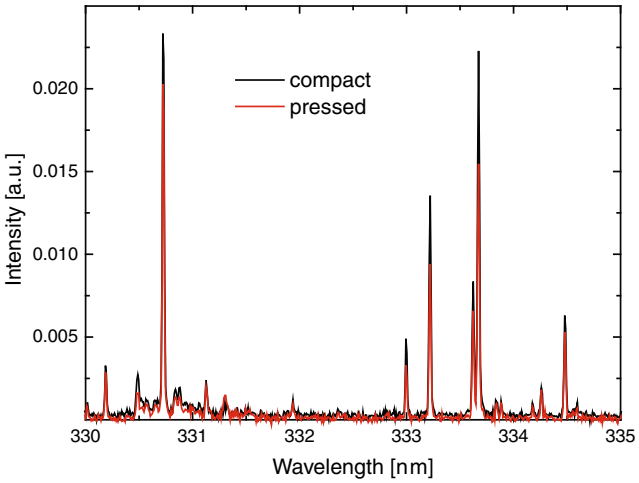

Fig. 2 Overlay of glow discharge optical emission spectrometry (GD-OES) spectra for compact and pressed powder samples; 18 mA, 2.24 hPa, 380 V, 4-mm anode diameter

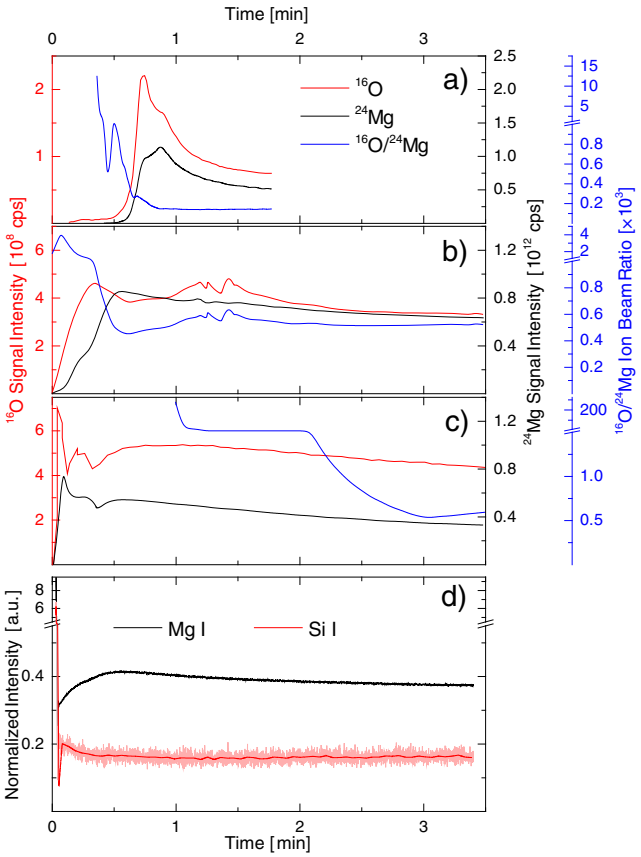

Fig. 3 Transient glow discharge mass spectrometry (GD-MS) signals of the matrix (magnesium) and the doping element (oxygen) for compact magnesium (*a*), pressed magnesium powder (325 mesh + 100–200 mesh, 1 + 1) (*b*), and sintered magnesium powder (approximately 10 % oxygen by mass) (*c*), and GD-OES signals for pressed magnesium powder doped with Si_3N_4 (silicon at approximately 1,500 mg·kg^{-1}) (*d*). The GD-MS signal profiles were measured with a low mass resolution ($m/\Delta m$~300) in the galvanostatic mode (70 mA, 320 mL min^{-1} argon flow rate) with an additional inductance coil. The GD-OES measurements were performed with a constant current and constant voltage (18 mA, 380 V, 4-mm anode diameter)

oxygen with the available experimental setup. With GD-OES, the analytical signals from both the matrix and the doping elements became stable a short time after initiation of the sputtering process, and the signal intensity remained constant during the whole measurement sequence (Fig. 3, panel d). From these observations it can be concluded that an acceptable degree of homogeneity was obtained. The same signal profiles from the matrix and doping elements (N, B) were also observed by GD-OES and GD-MS for pressed magnesium powder doped with BN or a mixture of BN, Si_3N_4, and MgO.

In Fig. 3 panels a–c it can be seen that the transient signals observed by fast flow GD-MS for both the matrix and the analyte exhibit complex profiles at the beginning of the sputtering process, followed by an exponential decay. However, the signal ratio (IBR) reaches a steady state and remains stable after 1–3 min of sputtering. The reason for these profiles might be the rather large inner area of the GD source and the interface (i.e., about 265 cm^2), which comes in contact with humid air each time a new sample is loaded.

GD-MS: effect of electrical parameters on the analytical signal

Initial measurements on magnesium highly doped with MgO indicated that, in this specific case, the use of the built-in power supply feeding the GD source is limited. In the galvanostatic mode (I=constant), even small additions of MgO led to instabilities of the signal with time and also to the frequent occurrence of spikes, especially in the low-intensity signals. This effect was also reproduced with another instrument of this type. Pressed magnesium samples doped with Si_3N_4 or a mixture of BN, Si_3N_4, and MgO and also pure compact magnesium exhibited stabler behavior. However, signal spikes and complex profiles from the transient signals were observed in this case as well. The reason for the spikes was found in a strong oscillation of the electrical parameters. In the case of oxide containing magnesium, the built-in power supply designed to level variations of the electrical discharge parameters was unable to operate at constant discharge current.

The underlying reason for the oscillations of the electrical parameters might be spark generation at the elevated argon pressure in the fast flow source, especially during the discharge ignition (transient discharge regime). The high current in the sparks (several amperes within nanosecond periods) causes electromagnetic disturbances in the ion-counting electronics.

An additional daisy-chained inductance coil (L=15 H) was installed to smoothen the electrical oscillations, leading to a satisfactory signal stability in the galvanostatic mode as well as in the potentiostatic mode (U=constant). However, the analysis of highly MgO doped samples was still not possible in the galvanostatic mode.

The current–voltage correlation and the effect of the GD voltage on the analytical signals (^{16}O, ^{24}Mg, and IBR) were investigated for three different magnesium samples—namely, compact bulk material, pressed undoped magnesium powder (325 mesh), and sintered Mg/MgO powder with the highest oxygen mass fraction (approximately 10 %)—using the built-in power supply and the inductance coil in the potentiostatic mode. The results obtained are shown in Fig. 4. The compact material and sintered powder show similar current–voltage profiles despite the fact that the oxygen content of the sintered powder was very high. For the sintered sample, an interesting behavior was observed. As soon as the sputtering started, we noticed a constant, voltage-independent IBR, although the signal intensities of magnesium and oxygen drop remarkably, which is in contradiction to the increasing current. To fully explain this signal drop at higher voltage, additional investigations are necessary. For samples with a higher oxygen content (pressed pellet, sintered compact), the dependence of the signal intensity of oxygen on the GD voltage has a clear inflection point corresponding to the onset of the sputtering process, whereas for compact material this dependence is almost linear, without any noticeable peculiarities.

GD-MS: calibration data

Since no reference data on the nonmetallic contents (except for silicon) were available either for the compact material or for the powders, a standard addition approach was applied to obtain calibration data. The measurement conditions are summarized in Table 2. The IBRs of $^{16}O^+$, $^{15}N^+$, $^{11}B^+$, and $^{29}Si^+$ to $^{24}Mg^+$ were used as the analytical responses. For potentiostatic measurements, the built-in power supply was used, and for galvanostatic measurements, an external power supply was used to overcome the limitations of the built-in device. By this means it was possible to measure all calibration samples in both modes. However, the discharge ignition required careful adjustment of both the voltage and the current. In principle, all measurements should be made under the same optimized conditions. Wherever possible we worked with the built-in hardware. As long as the signals are stable and there are no sparkovers, the final

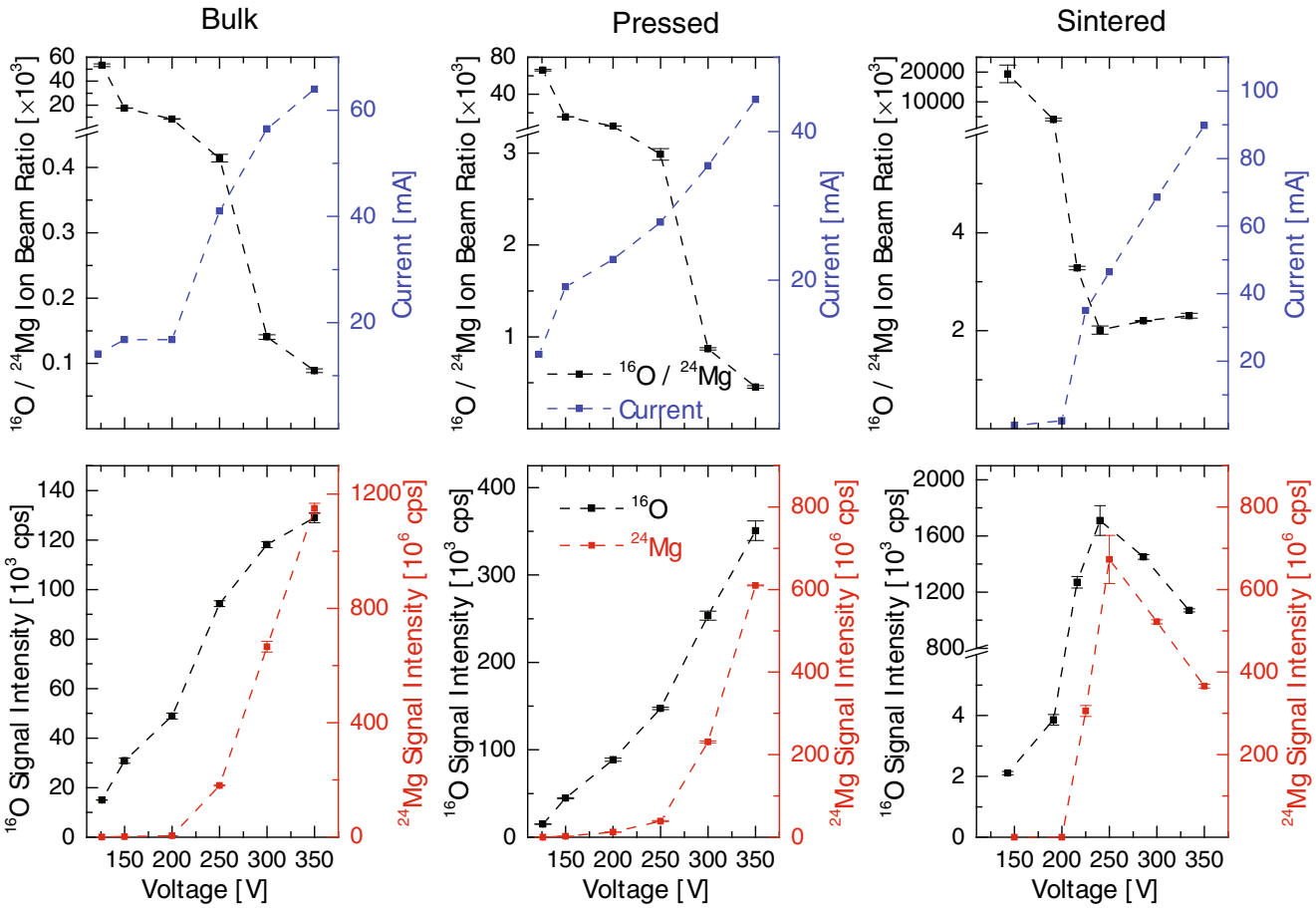

Fig. 4 Dependence of the discharge current and the signal intensity for magnesium and oxygen and the corresponding ion beam ratio (IBR) on the applied voltage for three different magnesium samples: bulk material; pressed powder (granularity 325 mesh); sintered magnesium and MgO mixture (oxygen mass fraction approximately 10 %; 2 g MgO and 6 g magnesium powder, 325 mesh). The measurements were performed using the built-in power supply with an inductance coil at an argon flow rate of 320 mL·min^{-1}. Values were recorded after a stabilization time of at least 3 min

Table 2 Experimental conditions

Spectrometer	ELEMENT GD (Thermo Fischer Scientific)
Resolution	4,000 (medium)
Discharge voltage (V)	250–350 (300 for potentiostatic mode)
Discharge current (mA)	10–70 (70 for galvanostatic mode)
Argon flow rate (mL·min^{-1})	320
Sampling time (ms)	20
Peltier cooling (°C)	4

Table 3 Determined oxygen content in magnesium powders used for fabrication of pressed and sintered samples

Magnesium powder	Determined oxygen mass fraction (%)
100–200 mesh	0.9±0.2
325 mesh	1.1±0.2
325 mesh used for sintering	1.7±0.3

conditions of the electrical parameters (U, I, and gas flow rate) are very similar in the potentiostatic and galvanostatic modes, although the means to achieve this can be difficult because of the different feedback characteristics. The results of the calibration experiments for oxygen are shown in Fig. 5. The calibrations for other nonmetallic dopants are provided in Fig 7.

No satisfactory calibration data could be obtained for the samples with high oxygen content if the GD source was operated in the potentiostatic mode (Fig. 5a). In the galvanostatic mode, calibration was possible within a relative spread of 10–30 %. The detection limit for an analytical procedure is directly determined by the uncertainty of the sensitivity and the uncertainty of the blank. The detection limits calculated according to [21] are within the range of thousands of micrograms per gram. Considering the remarkable linearity obtained, we can recommend the sintered powder standards for future applications for oxygen determination. In case of the pressed powder samples, the sensitivity (i.e., the slope of the calibration curve) depends on the granularity of the magnesium powder used, which may impose additional constraints on the use of pressed samples for calibration purposes. The measured oxygen contents in the undoped pressed and undoped sintered magnesium powder samples are within the low-percent region (Table 3) and depend on the granularity of the specific powders. The higher value for oxygen found for the magnesium powder used for fabricating the sintered samples may be explained by longer exposure to air.

During the sputtering of the samples with a high oxygen content, the extensive formation of oxygen-containing molecular species (O_2^+, MgO^+, ArO^+) was observed. However, only the IBR for O_2^+ correlates with the oxygen content for both sets of pressed powder samples and sintered samples (Fig. 6). The formation rate (expressed as IBR) for all the oxygen-containing polyatomic species shows a strong variation, especially in the case of the highest doped sample. The improvement of the calibration quality by accounting for oxygen losses due to the formation of polyatomic ions is, therefore, very difficult.

Calibration curves for the analytes boron, nitrogen, and silicon as obtained for magnesium powder (325 mesh) doped with a mixture of MgO, BN, and /Si_3N_4 are shown in Fig. 7. Good linearity of the calibration curves was obtained for boron and silicon, whereas the calibration quality for nitrogen was remarkably lower. In addition, the extrapolated value for the nitrogen content (2,700 mg·kg^{-1}) of the powder seems to be overestimated. The observed silicon content of the powder (300 mg·kg^{-1}) is in good agreement with the certified values for bulk material provided by the manufacturer. As certified values for the magnesium powder are not available, no further conclusions can be drawn with respect to this material.

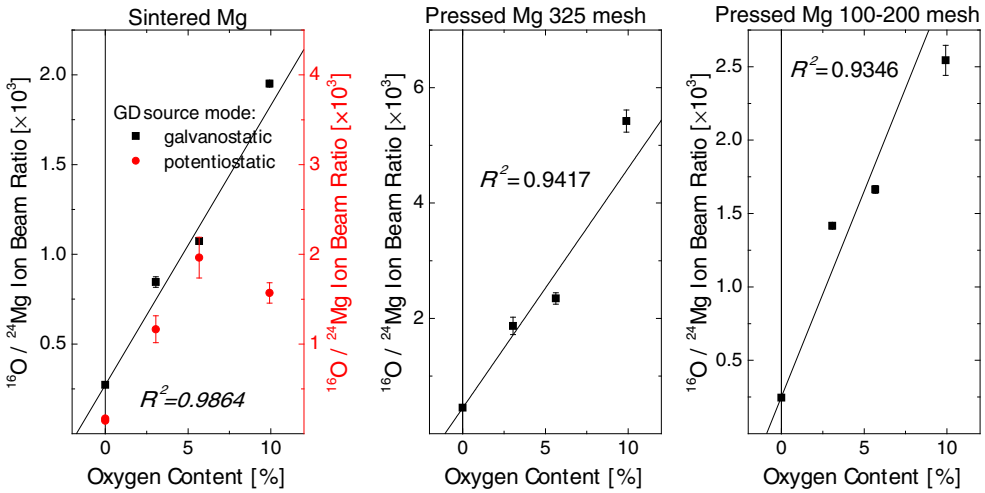

Fig. 5 Oxygen calibration data (IBR vs mass fraction) obtained by standard addition using an external power supply (with an inductance coil) in galvanostatic mode (70 mA, 320 mL·min^{-1} argon flow rate). The data obtained in the potentiostatic mode (300 V, 320 mL·min^{-1} argon flow) are shown only for sintered samples. However, pressed powder samples show a similar behavior

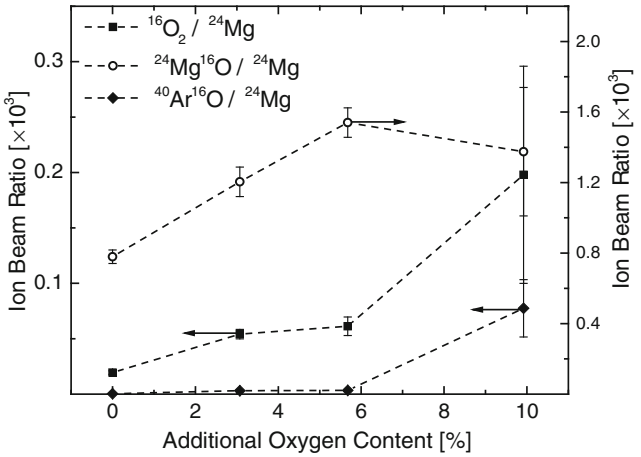

Fig. 6 IBRs for oxygen-containing polyatomic species measured during the analysis of MgO-doped pressed magnesium powder samples (granularity 100–200 mesh). Similar results were obtained for samples prepared from fine magnesium powder (granularity 350 mesh)

For samples fabricated from the finer magnesium powder (100–200 mesh) with the same dopant, the values were similar for boron and silicon. However, the calibration for nitrogen failed in this case for no clear reason.

For estimation of the matrix-specific RSFs for magnesium, pressed samples were used because the sintered samples did not include nonmetallic elements, other than oxygen. For elements such as boron and silicon, we expect only a small influence of the sample type on the RSF, as observed earlier for metallic impurities [21]. The magnesium-matrix-specific RSFs determined for boron, nitrogen, oxygen, and silicon obtained for the pressed powders are listed in Table 4. Although the values are not of the highest accuracy, comparison with the corresponding RSFs calculated from the SRSFs as provided by the instrument manufacturer shows huge differences, which demonstrates the necessity for matrix-adapted calibration even for semiquantitative determinations of nonmetallic impurities in magnesium. Notably, the SRSFs for oxygen and nitrogen are not known. However, more investigations are needed to determine the matrix-specific RSFs for nonmetallic impurities in magnesium with small uncertainty, which includes a full understanding of the behavior of samples with different morphology (pressed powders, sintered powders, and compact material).

Table 4 Relative sensitivity factors (RSFs) of investigated nonmetals in magnesium. The values in the *middle column* were calculated from the calibration data for pressed powder samples (325-mesh magnesium powder). The values in the *right column* were calculated using the standard RSF (*SRSF*) data (i.e., RSFs for iron matrix) as provided by the instrument manufacturer (Thermo Fischer Scientific) according to $RSF_{St}(X, Mg) = RSF(X, Fe)/RSF(Mg, Fe)$

Analyte X	RSF(X, Mg)	$RSF_{St}(X, Mg)$ based on SRSFs
B	21.4	4.3
N	131.3	–
O	24.0	–
Si	1.2	2.0

GD-MS: estimation of instrumental detection limits for oxygen

A first estimate of the detection limit related to the instrument can be made. The data obtained in the potentiostatic mode and in the galvanostatic mode can be combined, because the GD parameters used for the determination of the sensitivity and the background signal were very similar.

On the basis of the $3s$ criterion, with s being the standard deviation of the $^{16}O^+$ signal obtained for a magnesium sample under measurement conditions (350-V potentiostatic mode) where the discharge is operating but with no sputtering of the magnesium sample (i.e., no magnesium signal visible), the instrumental detection limit for oxygen in magnesium can be estimated according to

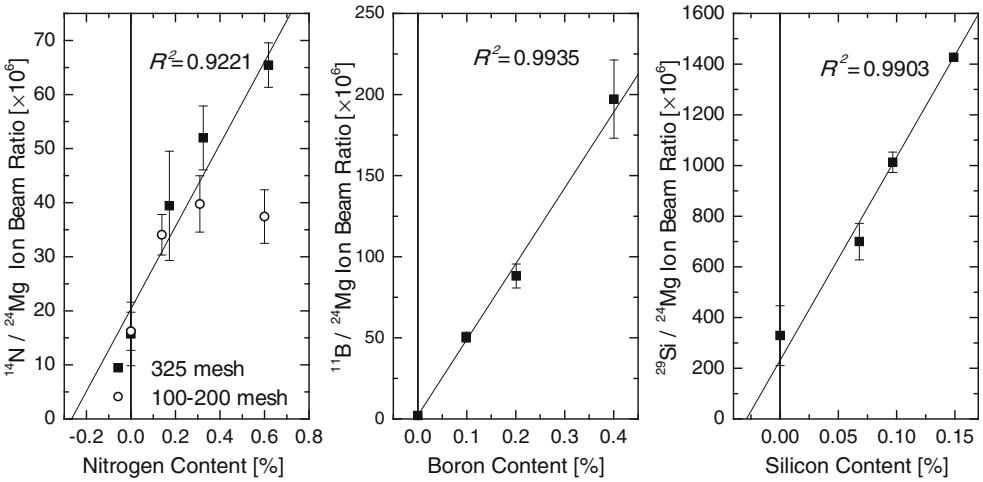

Fig. 7 GD-MS calibration data (IBR vs. mass fraction) for nitrogen, boron, and silicon obtained for a series of pressed magnesium powder samples (granularity of magnesium powder 325 mesh) doped with a mixture of MgO, BN, and Si_3N_4. The experimental conditions were the same as for the oxygen measurements

[22] to be approximately 500 $\mu g \cdot g^{-1}$. Although this value is an estimate of the order of magnitude, it provides an impression of the analytical performance of the fast flow GD source for the determination of oxygen in a complex matrix such as magnesium. This detection limit estimate significantly exceeds the measured values for oxygen in compact magnesium as obtained by a conventional GD source reported by Kikuta et al. [7], where detection limits were not reported. However, it should be noted that the time needed for the actual analysis by a conventional GD source is approximately five to ten times greater than for the fast flow GD source.

Conclusions

A method for the determination of oxygen, nitrogen, boron, and silicon in a magnesium matrix by GD-MS with a "fast flow" ion source has been successfully tested. However, owing to lack of reference data, a complete evaluation was not possible. Calibration data were obtained by using an external robust GD power supply with the ability to operate in the galvanostatic mode even under conditions where the built-in power supply failed. The use of an inductance coil in the cathode chain significantly increased the stability of the electrical discharge parameters, and consequently, the analytical signals obtained with both the internal and the external GD power supplies. The oxygen contents determined by standard addition for pressed magnesium powders are within the low-percent region, which is important when these powders are used for the preparation of calibration standards. Grain-size-dependent RSFs indicate that calibration for the analysis of powder samples with unknown granularity is more complex. Sintered samples showed better signal stability and linearity than pressed samples for the calibration of oxygen. Therefore, sintered samples appear to be more suitable for quantification purposes. A rough estimate of the instrument-related detection limit for oxygen significantly exceeds the reported oxygen contents as determined by means of GD-MS using a conventional low-pressure GD source.

The analysis of magnesium materials is very challenging. Even with the limitations described, the procedure applied allows a very fast simultaneous determination of nonmetallic impurities in magnesium matrices.

Acknowledgments Financial support by the European Metrology Research Programme (EMRP) is gratefully acknowledged (EMRP SIB09, "Primary Standards for Challenging Elements"). The EMRP is jointly funded by the EMRP-participating countries within EURAMET and the European Union.

References

1. Urbance RJ, Roth R, Clark J (2002) Magnesium market model simulation: the impact of increased automotive interest in magnesium. JOM 8:9
2. Haerle AG, Murray RW, Mercer WE, Mikucki BA, Miller MH (1997) The effect of non-metallic inclusions on the properties of die cast magnesium. SAE technical paper 970331. doi:10.4271/970331
3. Cochran CN, Belitskus DL, Kinosz DL (1977) Oxidation of aluminum-magnesium melts in air, oxygen, flue gas, and carbon dioxide. Metall Trans B 8(1):323–332. doi:10.1007/BF02657663
4. Tsuge A, Kanematsu W (2012) An analysis method for oxygen impurity in magnesium and its alloys: International standardization activity in parallel with R&D. Synthesiology 5(1): 25–35
5. Uemoto M (2011) Instrumental chemical analysis of magnesium and magnesium alloys. In: Czerwinski F (ed) Magnesium alloys - corrosion and surface treatments. InTech. doi:10.5772/13727
6. Tsuge A, Achiwa H, Morikawa H, Uemoto M, Kanematsu W (2011) Determination of oxygen content in magnesium and its alloys by inert gas fusion-infrared absorptiometry. Anal Sci 27(7):721–721
7. Kikuta E, Asano H, Kikuchi T (2007) Determination of oxygen in magnesium by glow discharge mass spectrometry. Tetsu To Hagane 93(2):128–131
8. Tartaglia J, Swartz R, Bentz R Jr, Howard J (2001) Magnesium alloy ingots: chemical and metallographic analyses. JOM 53(11):16–19. doi:10.1007/s11837-001-0187-4
9. Bakke P, Karlsen DO (1997) Inclusion assessment in magnesium and magnesium base alloys. SAE technical paper 970330. doi:10.4271/970330
10. Nakatsugawa I, Araki K, Takayasu H, Saito K, Matsusaka K, Endou T, Shida A (2003) Surface analysis of the injection molded magnesium alloy using GD-OES. Surf Coat Technol 169:307–310
11. Itoh S, Yamaguchi H, Hobo T, Kobayashi T (2004) Analysis of magnesium alloys by glow-discharge mass spectrometry. Bunseki Kagaku 53(6):569–574
12. Choi BH, You BS, Park IM (2006) Characterization of protective oxide layers formed on molten AZ91 alloy containing Ca and Be. Met Mater Int 12(1):63–67
13. Mykytiuk AP, Semeniuk P, Berman S (1990) Analysis of high-purity metals and semiconductor materials by glow discharge mass spectrometry. Spectrochim Acta Rev 13(1):1–10
14. Jakubowski N, Feldmann I, Stuewer D (1997) Grimm-type glow discharge ion source for operation with a high resolution inductively coupled plasma mass spectrometry instrument. J Anal Atom Spectrom 12(2):151–157. doi:10.1039/a604136a
15. Beyer C, Feldmann I, Gilmour D, Hoffmann V, Jakubowski N (2002) Development and analytical characterization of a Grimm-type glow discharge ion source operated with high gas flow rates and coupled to a mass spectrometer with high mass resolution. Spectrochim Acta B 57(10):1521–1533. doi:10.1016/S0584-8547(02)00106-4
16. Hoffmann V, Kasik M, Robinson P, Venzago C (2005) Glow discharge mass spectrometry. Anal Bioanal Chem 381(1):173–188. doi:10.1007/s00216-004-2933-2
17. Bogaerts A, Okhrimovskyy A, Gijbels R (2002) Calculation of the gas flow and its effect on the plasma characteristics for a modified Grimm-type glow discharge cell. J Anal Atom Spectrom 17(9):1076–1082. doi:10.1039/B200746K
18. ERM®-ED101 certificate of analysis (2004). BAM, Berlin
19. ERM®-ED102 certificate of analysis (2008). BAM, Berlin
20. Matschat R, Hinrichs J, Kipphardt H (2006) Application of glow discharge mass spectrometry to multielement ultra-trace

determination in ultrahigh-purity copper and iron: a calibration approach achieving quantification and traceability. Anal Bioanal Chem 386(1):125–141. doi:10.1007/s00216-006-0645-5

21. Hoffmann V, Jakubowski N, Stahlberg U, Stüwer D (1990) Vergleichende Untersuchungen zur Analyse kompakter und pulverförmiger Proben mittels Glimmentladungs-Massenspektrometrie (GD-MS). Analytische Glimmentladungsspektrometrie, KFA Jülich, pp 51–64
22. Hyk W, Stojek Z (2013) Quantifying uncertainty of determination by standard additions and serial dilutions methods taking into account standard uncertainties in both axes. Anal Chem 85(12):5933–5939. doi:10.1021/ac4007057